THE JOURNAL OF PHYSICAL CHEMISTRY A

Article

pubs.acs.org/JPCA

Face-Capping μ^3-BO in $B_6(BO)_7^-$: Boron Oxide Analogue of $B_6H_7^-$ with Rhombic 4c−2e Bonds

Jin-Chang Guo,[†,‡] Hai-Gang Lu,*[,†] Hua-Jin Zhai,[†] and Si-Dian Li*[,†]

[†]Institute of Molecular Science, Shanxi University, Taiyuan 030001, Shanxi, People's Republic of China

[‡]Institute of Materials Science and Department of Chemistry, Xinzhou Teachers' University, Xinzhou 034000, Shanxi, People's Republic of China

Supporting Information

ABSTRACT: Using the first-principle approaches, we predict a $B_6(BO)_7^-$ cluster with a face-capping μ^3-BO, which is the boron oxide analogue of *closo*-$B_6H_7^-$ with a face-capping μ^3-H. Detailed topological analysis of electron density clearly reveals the existence of three rhombic 4c−2e bonds around the B/H apex in both C_{3v} $B_6(BO)_7^-$ and C_{3v} $B_6H_7^-$, which possesses similar electron densities at their bond and ring critical points. The adaptive natural density partitioning (AdNDP) analysis provides a direct and visual picture of the B−B−B−B/H 4c−2e bonds for the first time. Adiabatic and vertical electron detachment energies of the concerned monoanions are calculated to facilitate their future photoelectron spectroscopy measurements and characterizations. The presence of the $B_6(BO)_7^-$ and $B_6H_7^-$ clusters extends the BO/H isolobal analogy to the whole μ^n-BO/H series (n = 1, 2, and 3) and enriches the chemistry of boronyl.

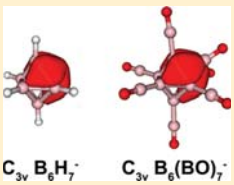

1. INTRODUCTION

Boron hydrides, the typical electron-deficient molecules, have attracted great attention from both theoretical and experimental chemists.[1,2] The novel multicenter bonds, such as the three-center−two-electron (3c−2e) bond in boranes, have played an essential role in advancing modern chemical bonding models.[3,4] However, four-center−two-electron (4c−2e) bonds of boranes have received scant attention.[5] Recently, the face-capping μ^3-H and 4c−2e bonding in polyhedral borane $[B_6H_7]^-$ received considerable attention in the literature.[6−8] Most notably, Hofmann et al. discovered three quasi-planar rhomboid B−B−B−H rings with the novel 4c−2e bonds in $B_6H_7^-$ based on topological analysis of electron density.[9,10] On the basis of the adaptive natural density partitioning (AdNDP) analysis, we also discovered the planar rhombic 4c−2e B−B−B−B σ-bonds in the two-dimensional boron α-sheet.[11] These fascinating structures and multicenter bonds of boranes and their derivatives originate from the electron deficiency of boron. It is therefore possible to synthesize the analogues of $B_6H_7^-$ with the rhombic 4c−2e B−B−B−B bonds.

On the basis of the isolobal analogy between terminal hydrogen (-H) and terminal boronyl (μ^1-BO) proposed in $C_n(BO)_n$ (n = 2−7),[12] we have successfully predicted and analyzed various boron-rich oxides, including the transition metal sandwich complexes,[13] the boronyl-substituted ethylenes and acetylenes,[14] the perfect tetrahedral $B(BO)_4^-$,[15] the cage-like $B_n(BO)_n^{2-}$ (n = 5−12),[16] the linear $B(BO)_2^-$, $B_2(BO)_2^-$, the triangular $B(BO)_3^-$, and the planar $B_3(BO)_n^-$ (n = 1,2), $B_4(BO)_n^-$ (n = 1−3), and $B_{10}(BO)^-$.[17−22] In 2010, Braunschweig et al. synthesized and characterized the first complex *trans*-$[(Cy_3P)_2BrPt(B{\equiv}O)]$ containing the terminal B≡O group.[23] Using a joint experimental and theoretical approach, our group also recently confirmed the existence of the bridging μ^2-BO groups in $B_2(BO)_3^-$ and $B_3(BO)_3^-$, which are analogous to the bridging μ^2-H in $B_2H_3^-$ and $B_3H_3^-$.[24] The existence of the face-capping μ^3-H in the polyhedral borane $[B_6H_7]^-$ presents the possibility of face-capping μ^3-BO in boron-rich boron oxide clusters to complete the μ^n-BO series (n = 1, 2, and 3) in H/BO analogy.

On the basis of the observation that $[B_6H_7]^-$ can be derived from the highly symmetric octahedral $B_6H_6^{2-}$ ion by adding a H^+ cation, the deltahedral *closo*-$B_6(BO)_7^-$ containing μ^3-BO may be similarly obtained by adding a BO^+ cation to $B_6(BO)_6^{2-}$, which had been predicted to be stable in gas-phase.[25] In this work, we investigate the possibility of $B_6(BO)_7^-$ with a face-capping μ^3-BO and analyze its bonding characteristics using both the adaptive natural density partitioning (AdNDP) approach and the Atoms-In-Molecules (AIM) theory.

2. THEORETICAL METHODS

Structural optimizations, frequencies analyses, natural bond orbital (NBO) analyses, and stability checks were performed using the hybrid B3LYP[26,27] and PBE0[28] methods with the standard Gaussian basis of 6-311+G(d,p).[29] The AIM analysis was performed using Multiwfn program.[30] Chemical bond partition of these species was performed utilizing the recently proposed AdNDP method[31−33] with the 6-31G(d,p) basis set (it has been shown that the AdNDP results are not sensitive to the level of theory or basis sets used). Adiabatic detachment energies (ADEs) were calculated as the energy differences between the ground-states of the anions and the corresponding neutrals, while vertical detachment energies (VDEs) were comparatively calculated with the time-dependent density

Received: September 7, 2013
Revised: October 20, 2013
Published: October 22, 2013

dx.doi.org/10.1021/jp4089723 | *J. Phys. Chem. A* 2013, 117, 11587−11591

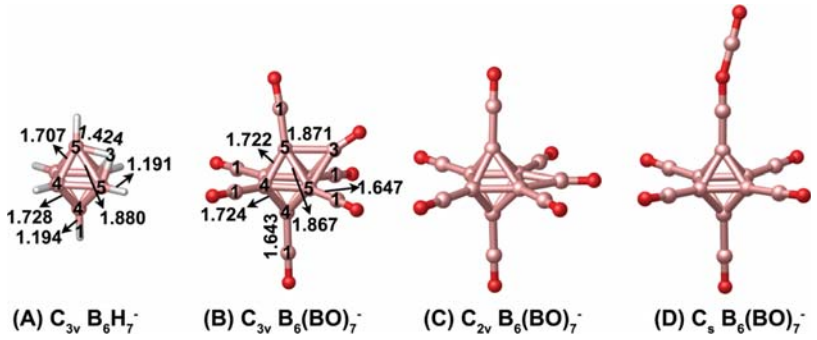

Figure 1. Geometric structures of C_{3v} $B_6H_7^-$ and C_{3v} $B_6(BO)_7^-$ with the selected bond lengths (Å) indicated at B3LYP. Equivalent μ^n-B/H atoms are labeled with the same number of n in panels A and B. Two important isomers (C,D) containing μ^1-BO and μ^2-BO are also listed for comparison with that in panel B.

Table 1. Natural Atomic Charges of μ^3-BO/H (q/lel), Wiberg Bond Indices of H/B^m–B^n ($WBI_{m\text{-}n}$), Total Valences of H/B^3 (Val), the Lowest Vibrational Frequencies (ν_{min}/cm^{-1}), and HOMO–LUMO Gaps (ΔE_{gap}/eV) of $B_6X_7^-$ (X = BO,H) at the B3LYP Level

		WBI_{1-4}	WBI_{1-5}	WBI_{4-4}	WBI_{4-5}	WBI_{5-5}	WBI_{3-5}	Val	ν_{min}	ΔE_{gap}
$B_6(BO)_7^-$	+0.16	0.90	0.90	0.63	0.65	0.49	0.39	3.13	+59	5.58
$B_6H_7^-$	+0.18	0.96	0.96	0.65	0.70	0.47	0.30	0.97	+368	5.36

functional theory (TD-DFT) procedure[34,35] and the outer valence Green's function (OVGF).[36,37] All DFT calculations in this work were carried out using the Gaussian 03 package.[38] Molecular structures and molecular orbitals were visualized using the CYLview[39] and Molekel 5.4[40] program, respectively.

3. RESULTS AND DISCUSSION

3.1. Geometrical Structures. Figure 1 shows the optimized geometries of C_{3v} $B_6H_7^-$ (Figure 1A) with a μ^3-H, C_{3v} $B_6(BO)_7^-$ (Figure 1B) with a μ^3-BO, C_{2v} $B_6(BO)_7^-$ (Figure 1C) with a bridging μ^2-BO, and C_s $B_6(BO)_7^-$ (Figure 1D) with the terminal BO at B3LYP level of theory. Because the PBE0 functional produces essentially the same structures for these species with only minor differences in bond lengths, we will mainly discuss the geometrical and electronic properties of the concerned species using the B3LYP functional in the following sections.

Among the three $B_6(BO)_7^-$ isomers, C_{3v} $B_6(BO)_7^-$, the analogue of the borane $B_6H_7^-$, is the most stable one without imaginary vibrational frequency on its potential energy surface. The C_{2v} and C_s structures are 0.42 and 0.44 eV less stable than the C_{3v} one at the CCSD(T)//B3LYP level, respectively. In particular, the C_{2v} isomer is a transition state with one imaginary vibrational frequency (56i cm^{-1}) leading the lowest-lying C_{3v} structure when fully relaxed. First-principle molecular dynamics (MD) simulations indicate that the C_{3v} $B_6(BO)_7^-$ isomers with the μ^3-BO at different B–B–B faces transfer between one another via C_{2v} transition states at 500 K.

In addition to μ^3-BO, there are three other types of B atoms with different coordination numbers in C_{3v} $B_6(BO)_7^-$. All the B atoms in C_{3v} $B_6(BO)_7^-$ can be classified into B^1 (μ^1-B in the terminal BO), B^3 (μ^3-B in the face-capping BO), B^5 (μ^5-B at the vertices face-capped by the μ^3-BO), and B^4 (μ^4-B on the face opposite to $B^5B^5B^5$). Among all B–B bonds, the terminal B^1–B^4 and B^1–B^5 bonds (1.643–1.647 Å) are the typical single bonds, and the B^4–B^4 and B^4–B^5 bonds (1.722–1.724 Å) are the normal skeletal bonds, while the B^5–B^5 (1.867 Å) and B^3–B^5 (1.871 Å) bonds are the weak skeletal bonds. Obviously, the B^3–B^5 and B^5–B^5 bonds are significantly longer than the other B–B bonds, and the elongation should significantly weaken their bonding strengthens. In addition, the B^3–B^5–B^5 triangles are almost coplanar with their B^5–B^5–B^4 triangular neighbors (the dihedral angles of B^3–B^5–B^5–B^4 are 178.98°). Thus, C_{3v} $B_6(BO)_7^-$ contains practically three equivalent B^3–B^5–B^5–B^4 planar rhombuses.

Beside the skeleton B–B bonds, there are seven terminal B–O bonds with lengths of 1.206–1.216 Å in the C_{3v} $B_6(BO)_7^-$ (Figure 1B). The six μ^1-BO bond lengths are 1.206 Å, which is typical for the B≡O triple bond,[17−19] and the face-capping μ^3-BO bond length is only slightly longer (1.216 Å) so that it should also be a triple bond.

3.2. Bonding Characteristics. The addition of BO^+/H^+, which produces three new B^3/H^3–B^5 bonds, modifies the octahedral skeleton of $B_6(BO)_7^-/B_6H_7^-$, especially the B^5–B^5 bonds in the capped $B^5B^5B^5$ face. The topological analysis of electron densities by Hofmann et al. shows that there are three equivalent quasi-planar rhombic H^3–B^5–B^5–B^4 rings with novel 4c–2e bonds in $B_6H_7^-$ from both the presence and the absence of the corresponding ring or bond critical points. As pointed by Jacobsen, however, these critical points alone do not directly relate to 4c–2e bonding. More direct descriptions of the 4c–2e bonding on the B^4–B^5–B^5–H^3/B^3 rhombuses would be therefore necessary and interesting.

The natural bond orbital (NBO) analyses (Table 1) can provide a direct insight on the bonding of the $B_6(BO)_7^-$. At first, the Wiberg bond index (WBI) indicates that the B^1–B^4 and B^1–B^5 bonds are the strongest B–B bonds (WBI = 0.90), and the skeletal B^4–B^4 and B^4–B^5 bonds are secondary (WBI = 0.63 and 0.65), while the B^5–B^5 and B^3–B^5 bonds are the weakest (WBI = 0.49 and 0.39). Obviously, the addition of BO^+ to the $B_6(BO)_6^{2-}$ cluster significantly weakens the B^5–B^5 bonds in the capped face. However, the total bond order of the combined B^5–B^5 and B^3–B^5 bonds are 0.88, which nearly equal that (0.90) of a B^1–B^5 bond. Consequently, the addition of BO^+ should form three combined 3c–2e B^3–B^5–B^5 bonds in the capping B^3–B^5–B^5–B^5 tetrahedron.

dx.doi.org/10.1021/jp4089723 | J. Phys. Chem. A 2013, 117, 11587–11591

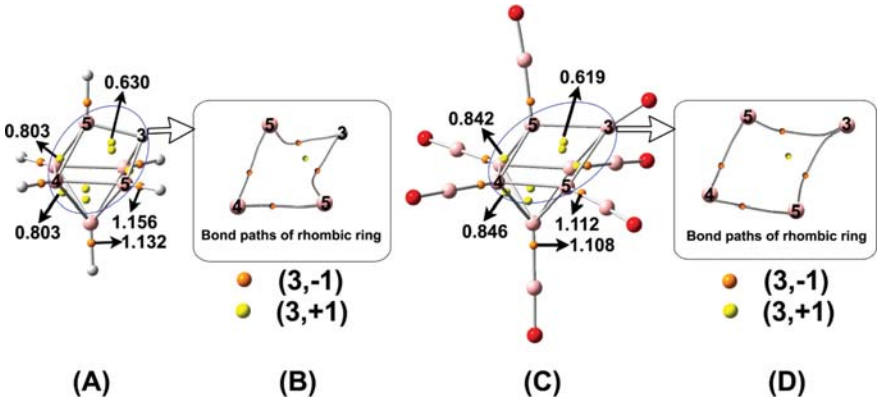

Figure 2. Topological AIM analysis of $B_6H_7^-$ (A, ref 9) and $B_6(BO)_7^-$ (C, at MP2/6-311+G(d) level) and their bond paths of rhombic $H^3-B^5-B^5-B^4$ (B) and $B^3-B^5-B^5-B^4$ (D) rings. The orange and yellow points stand for (3,−1) BCPs and (3,+1) RCPs, respectively.

Although the terminal μ^1-B−O and μ^3-B−O have the Wiberg bond orders of WBI = 1.90 and 1.77, their natural resonance theory (NRT) bond orders (including both covalent and ionic components) are 3.00 and 2.90, respectively; they are therefore triple bonds in nature, in agreement with the bonding characteristic predicted from their bond lengths. In their NRT bond orders, the covalent and ionic components are 1.78 and 1.22 for μ^1-B≡O and 1.64 and 1.26 for μ^3-B≡O, respectively, indicating that such B≡O triple bonds possess considerable ionic characteristics. Because both the Wiberg bond order and NRT covalent component of μ^3-B≡O are less than those of μ^1-B≡O, the covalent bonding of μ^3-B≡O is clearly weaker than that of μ^1-B≡O. However, there are three μ^3-B−B bonds (WBI = 0.39) for μ^3-B and only one μ^1-B−B bond (WBI = 0.90) for μ^1-B in the $B_6(BO)_7^-$ so that the overall covalency of μ^3-B (2.94) is more than that of μ^1-B (2.80). Therefore, the face-capping μ^3-B has more covalent bonding characteristics than the terminal μ^1-B.

According to Bader's AIM theory, the analysis of the electron density can be used to define critical points that indicate a bonding situation. Similar to the AIM analyses of $B_6H_7^-$ (Figure 2A,B), there is no (3,−1) bond critical points (BCPs) between B^5-B^5 atoms, while there are three equivalent (3,+1) $B^3-B^5-B^5-B^4$ ring critical points (RCPs) in C_{3v} $B_6(BO)_7^-$ (Figure 2C,D). The RCP electron densities in three quasi-planar $B^3-B^5-B^5-B^4$ rhomboids of $B_6(BO)_7^-$ are 0.619 |e|, well comparable with the corresponding value of 0.630 |e| in C_{3v} $B_6H_7^-$. Therefore, the three 3c−2e $B^3-B^5-B^5$ bonds should be extended to form three rhombic $B^3-B^5-B^5-B^4$ 4c−2e bonds in $B_6(BO)_7^-$.

AdNDP analyses provide a direct and visual description of the rhombic $B^3-B^5-B^5-B^4$ 4c−2e bonds in $B_6(BO)_7^-$ and have been successfully used for the three-dimensional structures of the tetrahedral B_4H_4 and the octahedral $B_6H_4^-$ clusters by Olson and Boldyrev.[41,42] The localized molecular orbitals found by the AdNDP analyses of $B_6H_7^-$ and $B_6(BO)_7^-$, were listed in Figure 3. In $B_6H_7^-$ (Figure 3I), there are six 2c−2e B−H bonds, one $B^4-B^4-B^4$ 3c−2e bond, and three $B^4-B^4-B^5$ 3c−2e bonds. In $B_6(BO)_7^-$, there are three B^1-B^4 and three B^1-B^5 2c−2e bonds, one $B^4-B^4-B^4$ 3c−2e bond, three $B^4-B^4-B^5$ 3c−2e bonds, seven B^1−O 2c−2e bonds (B≡O triple bonds, including σ and π bonds), and 14 oxygen lone pairs. Obviously, these two groups of localized molecular orbitals are C_{3v} symmetry-adapted in $B_6H_7^-$ and $B_6(BO)_7^-$. However, in such a bonding pattern, there are still 6.38 and 7.06 electrons remaining as residues.

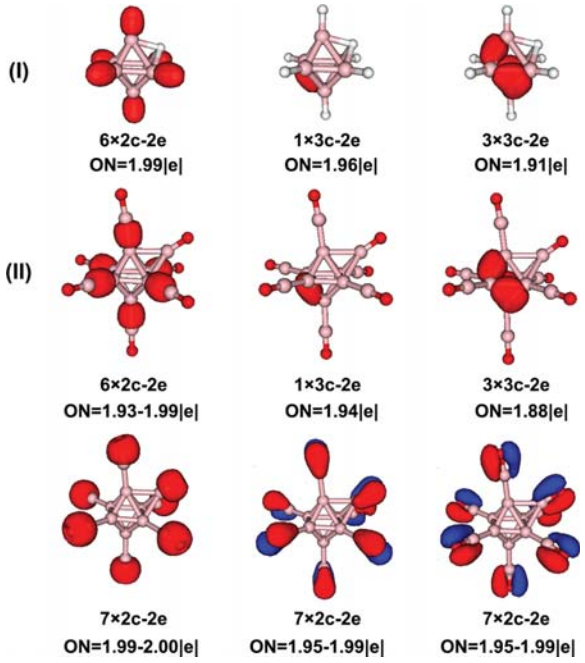

Figure 3. The 2c−2e and 3c−2e localized molecular orbitals of C_{3v} $B_6H_7^-$(I) and $B_6(BO)_7^-$(II) obtained by AdNDP analyses. The ON denotes the occupation numbers on the localized orbitals.

The remaining electrons can be projected into three localized orbitals with five possible symmetry-adapted AdNDP schemes (see Figure 4I and II), i.e., three 2c−2e B^5-B^5 or B^3-B^5 bonds, three 3c−2e $B^3-B^5-B^5$ or $B^5-B^5-B^4$ bonds, or three equivalent 4c−2e $B^3-B^5-B^5-B^4$ interactions (Figure 4II). The projected electron occupation numbers (ON) on the localized orbitals can be taken as a criterion to evaluate the reliability of different AdNDP schemes. The ONs of the two 2c−2e schemes are only 1.16 and 1.39 on the B^5-B^5 and B^3-B^5 bonds in $B_6(BO)_7^-$, far less than the empirical minimum ON (1.60), so that both 2c−2c schemes must be discarded. In the two 3c−2e schemes, their ONs are 1.68 and 1.71 on the $B^3-B^5-B^5$ and $B^5-B^5-B^4$ bonds, suggesting that both 3c−2e schemes are possible. The almost same ONs (1.68 and 1.71) for the two 3c−2e schemes demonstrate that both the B^3 and

dx.doi.org/10.1021/jp4089723 | J. Phys. Chem. A 2013, 117, 11587−11591

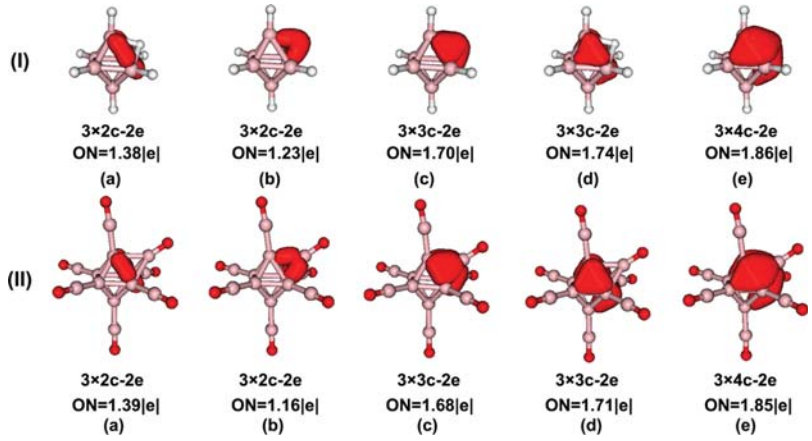

Figure 4. Five possible symmetry-adapted AdNDP bonding patterns of C_{3v} $B_6H_7^-$ (I) and $B_6(BO)_7^-$ (II). The ON denotes the occupation numbers on the localized orbitals.

B^4 atoms are equally weighted in the multicenter bonding of the AdNDP analysis. This indicates that the more reliable symmetry-adapted multicenter bonds should include three equivalent 4c−2e B^3−B^5−B^5−B^4 bonds in $B_6(BO)_7^-$, as shown by the AIM analyses in Figure 4II. Such 4c−2e B^3−B^5−B^5−B^4 bonds turn out to possess the highest values of ON = 1.85 and therefore represent the most reliable bonding scheme. As shown in Figure 4I, the 4c−2e H^3−B^5−B^5−B^4 bonds in $B_6H_7^-$ proposed by Hofmann et al. are also well described by the AdNDP approach.

Similarly, there are some other possible clusters analogous to the $B_6H_7^-$ and $B_6(BO)_7^-$. Figure 5 shows the optimized

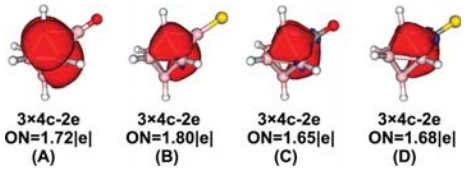

Figure 5. The 4c−2e localized molecular orbitals in $B_6H_6(\mu^3\text{-BO})^-$ (A), $B_6H_6(\mu^3\text{-BS})^-$ (B), C_{3v} $B_6H_6(\mu^3\text{-CO})$ (C), and $B_6H_6(\mu^3\text{-CS})$ (D). The ON values denote the occupation numbers of the localized orbitals.

structures of the face-capping C_{3v} $B_6H_6(\mu^3\text{-BO})^-$, C_{3v} $B_6H_6(\mu^3\text{-BS})^-$, C_{3v} $B_6H_6(\mu^3\text{-CO})$, and C_{3v} $B_6H_6(\mu^3\text{-CS})$ at the B3LYP level. As the singlet substitutes $B_6H_7^-$, they are also the true minima of the systems with three equivalent rhombic B^4−B^5−B^5−B^3 (or C^3) 4c−2e bonds (Figure 5).

3.3. Possible Synthesized Pathways, ADE and VDE.

The C_{3v} $B_6(BO)_7^-$ cluster could be synthesized in two possible pathways: (1) $B_6(BO)_6^{2-} + BO^+ = B_6(BO)_7^-$ and (2) $B_6H_7^- + 7BO = B_6(BO)_7^- + 3/2H_2$. Both reactions are strongly exothermic and their standard enthalpies are −328.7 and −993.7 kcal/mol (including ZPE correction) at the B3LYP levels, respectively. This demonstrates that the formation of $B_6(BO)_7^-$ is an irreversible processes. In addition, as shown in Table 1, C_{3v} $B_6(BO)_7^-$ possess a relatively large HOMO−LUMO energy gap (ΔE_{gap} = 5.58 eV), so the product is expected to be highly stable in thermodynamics.

In order to facilitate future photoelectron spectroscopy (PES) characterizations of the C_{3v} $B_6(BO)_7^-$ and $B_6H_7^-$ structures, their theoretical ADE and the first two VDEs are calculated using both TD-DFT and OVGF(full) methods. For these species, the first VDE(X) corresponds to detaching one electron vertically from the degenerate HOMO(e) with the final state of $^2A''$, while the second VDE(A) corresponds to detaching one electron vertically from the HOMO−1(a_1) with the final state of $^2A'$. For C_{3v} $B_6(BO)_7^-(^1A_1)$, as shown in Table 2, its calculated one-electron detachment energies are ADE = 7.58 eV, VDE(X) = 7.75 eV, and VDE(A) = 8.25 eV at the TD-B3LYP level, respectively. These unusually high values[12−23] suggest again that C_{3v} $B_6(BO)_7^-$ is highly stable in thermodynamics and possible to be synthesized in future experiments. In addition, the ADE and VDE values at the PBE0 level are very close to those at the B3LYP level (Table 2). Interestingly, OVGF calculations for these monoanions also produce VDE values well comparable with the TD-DFT method at both B3LYP and PBE0 geometries (see Table 2).

Table 2. Calculated Low-Lying ADE and VDE Values (eV) of C_{3v} $B_6(BO)_7^-$ and $B_6H_7^-$ at Various Levels

			B3LYP		PBE0	
		final state[a]	TDDFT	OVGF[b]	TDDFT	OVGF[b]
C_{3v} $B_6(BO)_7^-$ ($^1A_1$)	ADE		7.58		7.75	
	VDE(X)	$^2A''$	7.75	7.49(0.90)	7.89	7.51(0.90)
	VDE(A)	$^2A'$	8.25	8.22(0.90)	8.42	8.27(0.90)
C_{3v} $B_6H_7^-$ ($^1A_1$)	ADE		3.87		3.95	
	VDE(X)	$^2A''$	4.23	4.16(0.90)	4.30	4.17(0.90)
	VDE(A)	$^2A'$	4.85	4.89(0.90)	4.96	4.95(0.90)

[a]The first and second excited states of these anions use C_s descriptions because their real electronic structures possess C_s symmetry due to John−Teller distortions. [b]Values in parentheses represent the pole strength values from the OVGF approach.

dx.doi.org/10.1021/jp4089723 | J. Phys. Chem. A 2013, 117, 11587−11591

The high pole strengths (>0.88) of the electron detachment channels for $B_6X_7^-$ (X = BO,H) strongly suggest that multireference interactions is most likely negligible for the monoanions concerned in this work.

4. SUMMARY

We have presented in this work strong theoretical evidence for the possible existence of $B_6(BO)_7^-$ with a face-capping μ^3-BO to complete the μ^n-BO series (n = 1, 2, and 3) in BO/H analogy. Detailed NBO, AIM, and AdNDP analyses provide direct and visual descriptions for the novel delocalized 4c−2e σ-bonds of rhombic B−B−B−B and B−B−B−H rings in $B_6(BO)_7^-$ and polyhedral borane $B_6H_7^-$, respectively. The designed synthesized pathways suggest that the $B_6(BO)_7^-$ cluster are thermodynamically possible to be produced in experiments. The adiabatic and vertical electron detachment energies of these monoanions are predicted to facilitate their future experimental characterizations.

■ ASSOCIATED CONTENT

Supporting Information

AdNDP bonding patterns of $B_6H_6(BO)^-$ (a) and C_{3v} $B_6H_6(BS)^-$ (b), C_{3v} $B_6H_6(CO)$ (c), and $B_6H_6(CS)$ (d); optimized structures of C_{3v} $B_6X_7^-$ and C_{3v} $B_6H_6X^-$ (X = BO, BS, and H) both at B3LYP and PBE0 levels with their atomic coordinates, total DFT energies (including zero-point energy/Hartree), and the lowest vibrational frequencies indicated. This material is available free of charge via the Internet at http://pubs.acs.org.

■ AUTHOR INFORMATION

Corresponding Authors

*(H.-G.L) E-mail: haiganglu@yahoo.com.
*(S.-D.L.) E-mail: lisidian@sxu.edu.cn.

Notes

The authors declare no competing financial interest.

■ ACKNOWLEDGMENTS

This work was supported by the Natural Science Foundation of China (No.20873117) and (No.21243004).

■ REFERENCES

(1) Shore, S. G. In *Boron Hydride Chemistry*; Muetterties, E. L., Ed.; Academic Press: New York, 1975.
(2) Cotton, F. A.; Wilkinson, G.; Murrillo, C. A.; Bochmann, M. *Advanced Inorganic Chemistry*, 6th ed.; Wiley: New York, 1999.
(3) Lipscomb, W. N. *Boron Hydrides*; Benjamin: New York, 1963.
(4) Lipscomb, W. N. *Science* **1977**, *196*, 1047−1055.
(5) Harcourt, R. D. *J. Phys. Chem.* **1991**, *95*, 6916−6918.
(6) McKee, M.; Biihl, M.; Charkin, P.; Schleyer, P. v. R. *Inorg. Chem.* **1993**, *32*, 4549−4554.
(7) Forster, D.; Scheins, S.; Luger, P.; Lentz, D.; Preetz, W. *Eur. J. Inorg. Chem.* **2007**, 3169−3172.
(8) Jacobsen, H. *Dalton Trans.* **2009**, 4252−4258.
(9) Hofmann, K.; Prosenc, M. H.; Albert, B. R. *Chem. Commun.* **2007**, 3097−3099.
(10) Balakrishnarajan, M. M.; Hoffmann, R. *J. Am. Chem. Soc.* **2004**, *126*, 13119−13131.
(11) Galeev, T. R.; Chen, Q.; Guo, J. C.; Bai, H.; Miao, C. Q.; Lu, H. G.; Sergeeva, A. P.; Li, S. D.; Boldyrev, A. I. *Phys. Chem. Chem. Phys.* **2011**, *13*, 11575−11578.
(12) Li, S. D.; Miao, C. Q.; Guo, J. C.; Ren, G. M. *J. Comput. Chem.* **2005**, *26*, 799−802.
(13) Ren, G. M.; Li, S. D.; Miao, C. Q. *J. Mol. Struct.: THEOCHEM* **2006**, *770*, 193−197.
(14) Li, S. D.; Guo, J. C.; Ren, G. M. *J. Mol. Struct.: THEOCHEM* **2007**, *821*, 153−159.
(15) Yao, W. Z.; Guo, J. C.; Lu, H. G.; Li, S. D. *J. Phys. Chem. A* **2009**, *113*, 2561−2564.
(16) Miao, C. Q.; Li, S. D. *Sci. China: Chem.* **2011**, *54*, 756−761.
(17) Zhai, H. J.; Wang, L. M.; Li, S. D.; Wang, L. S. *J. Phys. Chem. A* **2007**, *111*, 1030−1035.
(18) Zhai, H. J.; Li, S. D.; Wang, L. S. *J. Am. Chem. Soc.* **2007**, *129*, 9254−9255.
(19) Li, S. D.; Zhai, H. J.; Wang, L. S. *J. Am. Chem. Soc.* **2008**, *130*, 2573−2579.
(20) Zhai, H. J.; Miao, C. Q.; Li, S. D.; Wang, L. S. *J. Phys. Chem. A* **2010**, *114*, 12155−12161.
(21) Chen, Q.; Zhai, H. J.; Li, S. D.; Wang, L. S. *J. Chem. Phys.* **2012**, *137*, 0443071−0443077.
(22) Chen, Q.; Bai, H.; Zhai, H. J.; Li, S. D.; Wang, L. S. *J. Chem. Phys.* **2013**, *139*, 044308.
(23) Braunschweig, H.; Radacki, K.; Schneider. *Science* **2010**, *328*, 345−347.
(24) Zhai, H. J.; Guo, J. C.; Li, S. D.; Wang, L. S. *ChemPhysChem* **2011**, *12*, 2549−2553.
(25) Zint, N.; Dreuw, A.; Cederbaum, L. S. *J. Am. Chem. Soc.* **2002**, *124*, 4910−4917.
(26) Becke, A. D. *J. Chem. Phys.* **1993**, *98*, 5648−5652.
(27) Lee, C.; Yang, W.; Parr, R. G. *Phys. Rev. B* **1988**, *37*, 785−789.
(28) Perdew, J. P.; Chevary, J. A. S.; Vosko, H.; Jackson, K. A.; Pederson, M. R.; Singh, D. J.; Fiolhais, C. *Phys. Rev. B* **1992**, *46*, 6671−6687.
(29) Miehlich, B.; Savin, A.; Stoll, H.; Preuss, H. *Chem. Phys. Lett.* **1989**, *157*, 200−206.
(30) Lu, T.; Chen, F. *J. Comput. Chem.* **2011**, *33*, 580−592.
(31) Zubarev, D. Y.; Boldyrev, A. I. *Phys. Chem. Chem. Phys.* **2008**, *10*, 5207−5217.
(32) Zubarev, D. Y.; Boldyrev, A. I. *J. Org. Chem.* **2008**, *73*, 9251−9258.
(33) Zubarev, D. Y.; Boldyrev, A. I. Deciphering Chemical Bonding in Golden Cages. *J. Phys. Chem. A* **2009**, *113*, 866−868.
(34) Casida, M. E.; Jamorski, C.; Casida, K. C.; Salahub, D. R. *J. Chem. Phys.* **1998**, *108*, 4439−4449.
(35) Stratmann, R. E.; Scuseria, G. E.; Frisch, M. J. *J. Chem. Phys.* **1998**, *109*, 8218−8224.
(36) Ortiz, J. V. *J. Chem. Phys.* **1988**, *89*, 6348−6352.
(37) Ortiz, J. V.; Zakrzewski, V. G.; Dolgounircheva, O. *Conceptual Perspectives in Quantum Chemistry*; Kluwer Academic: Norwell, MA, 1997.
(38) Frisch, M. J.; et al. *Gaussian 03*, revision E.01; Gaussian, Inc.: Pittsburgh, PA, 2003.
(39) Legault, C. Y. *CYLview*, 1.0; Université de Sherbrooke: Sherbrooke, Canada, 2009.
(40) Varetto, U. *Molekel*, version 5.4.0.8; Swiss National Supercomputing Centre: Manno, Switzerland, 2009.
(41) Olson, J. K.; Boldyrev, A. I. *J. Phys. Chem. A* **2013**, *117*, 1614−1620.
(42) Olson, J. K.; Boldyrev, A. I. *Chem. Phys.* **2011**, *379*, 1−5.